Iron-naphthalenedicarboxylic acid gels and their highly efficient arsenic (V) removal†

Jianfei Sui, Lihuan Wang, Wenrong Zhao, and Jingcheng Hao*

Key Laboratory of Colloid and Interface Chemistry& Key Laboratory of Special Aggregated Materials, Shandong University, Ministry of Education, Jinan 250100, P. R. China

* Corresponding author. Tel.: +86-531-88366074, Fax: +86-531-88564750
E-mail: jhao@sdu.edu.cn

I. Experimental section

I.1. Chemicals and materials. $Fe(NO_3)_3 \cdot 6H_2O$ and thiourea were purchased from Shantou Xilong Chemical Factory. NaOH and ascorbic acid were purchased from Sinopharm Chemical Reagent Co. Ltd. Ethanol was purchased from Tianjin Fuyu Fine Chemical Co. Ltd. $NaNO_3$ was purchased from Tianjin Kermel Chemical Reagent Development Centre. HCl was purchased from Lai Yang Kangde Chemical Co., Ltd. Na_3AsO_4 was purchased from Shanghai Beizhou Biotechnology Co. Ltd. All the chemicals were analytical reagent grade (A.R.). 1,4-Naphthalenedicarboxylicacid (95%) was purchased from Aladdin Chemistry Co. Ltd. All the chemicals were used without further treatment. Ultrapure water with a resistivity of 18.25 MΩ·cm was obtained froma UPH-IV ultrapure water purifier (China).

I.2 Gelation behavior study. First, 0.2 mmol NDC was dissolved in 2 mL of ethanol at high temperature. Then a series of $Fe(NO_3)_3$ with different amounts were dissolved in 2 mL of ethanol. MOG formed by mixing the above two solutions.

I.3 Field-emission scanning electron microscopy (FE-SEM) observations. For SEM observations, about 2 μL of gel sample was dropt on a silica wafer surface, and most of the colloid gel was removed using small forceps to form a thin film. The wafers were freeze-dried under vacuum. The samples were observed on JEOL JSM-6700F FE-SEM at 3 kV.

I.4 Rheological measurements. The rheological measurements were carried out on a HAAKE RS6000 rheometer with a cone-plate system (C35/1TiL07116) for samples with high viscosity. In oscillatory measurements, an amplitude sweep at a fixed frequency of 1 Hz was carried out prior to the following frequency sweep in order to ensure the selected stresswas in linear viscoelastic region.

I.5 Fourier transform infrared spectroscopy (FT-IR) measurements. The

FT-IR spectra were measured on a VERTEX-70/70v FT-IR spectrometer (Bruker Optics, Germany). Spectra over 4000-400 cm^{-1} were obtained by taking 64 scans with a final resolution of 4 cm^{-1}. Spectral manipulation was performed by the OPUS 6.5 software package (Bruker Optics, Germany).

I.6 Adsorption isotherm. To perform the adsorption reaction, the Fe-NDC MOGs were freeze-dried under vacuum to obtain the xerogels. For a typical process, 10 mg xerogel was submerged to 50 mL sodium arsenate solution with a series of concentration at 2, 5, 10, 15, 20, 30, 40, 60 $mg \cdot L^{-1}$ (pH = 7.0 ± 0.1, 0.01 $mol \cdot L^{-1}$ $NaNO_3$ was used as background dielectric) and the mixtures were kept stirring for 24 h. The solution was then filtered with 0.22 μm filter membrane. Filtrate was collected and analyzed by Atomic Fluorescence Spectrophotometer (AFS-930, Beijing Titan Instruments Co., Ltd.). The amount of arsenate adsorbed was calculated using the following *Eq*. 1:

$$q_e = (c_0 - c_e)\frac{V}{w} \quad (1)$$

where q_e is the adsorption capacity ($mg \cdot g^{-1}$) at equilibrium, C_0 and C_e are the initial and equilibrium liquid-phase concentrations of arsenate ($mg \cdot L^{-1}$), respectively, V is the volume of solution (L) and w is the mass (g) of adsorbent used.

I.7 Adsorption kinetics. 50 mg xerogel and 250 mL of arsenate solution (30 $mg \cdot L^{-1}$, pH = 7.0 ± 0.1, 0.01 $mol \cdot L^{-1}$ $NaNO_3$ was used as background dielectric) were added to beaker and the mixture was kept stirring for 24 h. Samples were taken at predetermined intervals and contents were filtered by 0.22 μm filter membrane and filtrate was collected and analyzed by AFS.

I.8 Arsenic analysis. To analyse the concentration of As(V) in the solution, As (V) was reduced to As (III). 1 mL filtrate,1 mL concentrated hydrochloric acid,1 mL 10% thiourea and 10% ascorbic acid aqueous solution were mixed for 30 min to

transform As (V) to As (III). As(III) was analyzed using Atomic Fluorescence Spectrophotometer (AFS-930, Beijing Titan Instruments Co., Ltd.).

II. Models used in this paper

II.1 Langmuir isotherm model. Langmuir isotherm *Eq*. is derived from simple mass kinetics. The *Eq*. 1 is obtained by assuming three conditions: i) no lateral interaction exsits among the molecules; ii) uniform energies of adsorption were applied onto the surface; iii) no transmigration of adsorbate occurs in the plane of the surface. The Langmuir *Eq*. 2 can be represented as follows:[1]

$$\frac{1}{q_e} = \frac{1}{K_L q_m c_e} + \frac{1}{q_m} \qquad (2)$$

where q_e is the amount of adsorbate adsorbed per unit weight of the adsorbent at equilibrium ($mg \cdot g^{-1}$), q_m is the maximum adsorption capacity ($mg \cdot g^{-1}$), K_L is the Langmuir constant, c_e is the equilibrium concentration of the adsorbate in solution ($mg \cdot L^{-1}$).

II.2 Freundlich isotherm model. The Freundlich isotherm *Eq*. is derived for describing multilayer adsorption equilibrium on heterogeneous adsorbent surface with non-identical sites. This model assumes that the rate of decrease of the fraction of the surface is unoccupied by the adsorbate molecules is proportional to a certain power of the partial pressure of the adsorbate. The Freundlich isotherm *Eq*. 3 can be represented as follows:[2]

$$\ln q_e = \frac{1}{n} \ln C_e + \ln K_F \qquad (3)$$

where q_e and c_e have the same meanings as that of *Eq*. 1, K_F is the Freundlich constant, n is the Freundlich constant, which reflects adsorption intensity.

II.3 The pseudo-first-order kinetic model. The pseudo-first-order kinetic model also known as Lagergren and Svenska *Eq*. 4 can be represented as follows:[3]

$$\ln(q_e - q_t) = \ln q_e - k_1 t \quad (4)$$

where q_e and q_t are the amounts of arsenic adsorbed (mg·g^{-1}) at equilibrium and at any time t (min), respectively, and k_1 is the rate constant of adsorption (min^{-1}). Values of k_1 were calculated from the plots of ln (q_e - q_t) *vs*. *t*.

II.4 The pseudo-second-order kinetic model. This model is also used to predict the kinetic parameters, the *Eqs*. 5 and 6 can be represented as:[4]

$$\frac{t}{q_t} = \frac{1}{h} + \frac{t}{q_e} \quad (5)$$

and

$$h = k_2 q_e^2 \quad (6)$$

where q_e and q_t are the amounts of arsenic adsorbed (mg·g^{-1}) at equilibrium and at any time t (min), h is the initial sorption rate (mg·g^{-1}·min^{-1}). The values of q_e (1/slope), k_2 (slope^2/intercept), and h (1/intercept) can be calculated from the plots of t/q_t vs. t.

II.5 The calculation of Gibbs Free Energy (ΔG^0)

The Gibbs free energy (ΔG^0) is calculated from the *Eq*.:

$$\Delta G^0 = -RT\ln K_L \quad (7)$$

where R is the ideal gas constant, T (K) is the absolute temperature and K_L is the Langmuir constant. The ΔG^0 calculated using the Langmuir constant (K_L) is -28.495 kJ·mol^{-1}, indicating that the arsenic adsorption is spontaneous.

III. Supplementary Figures and Tables

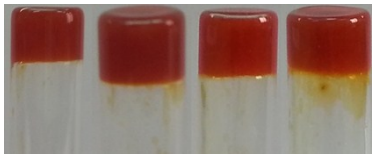

Fig. S1 Photographs of typical samples after 24 h. c_{NDC} = 100 mmol·L^{-1} and $c_{Fe^{3+}}$ (from left to right) = 75, 100, 125, 150 mmol·L^{-1}, respectively.

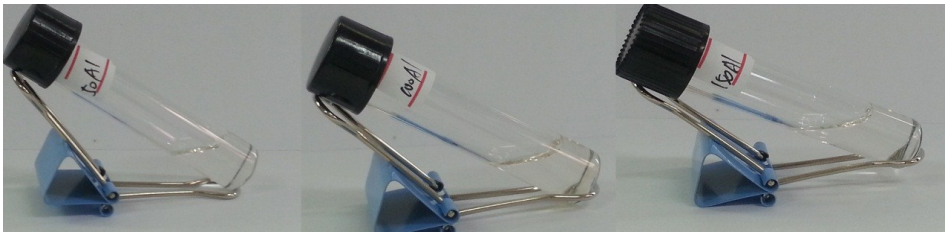

Fig. S2 Photographs of typical samples after 48 h. c_{NDC} = 100 mmol·L^{-1} and c_{Al}^{3+} (from left to right) = 50, 100, 150 mmol·L^{-1}, respectively.

Fig. S3 Photographs of typical samples after 48 h. c_{NDC} = 100 mmol·L^{-1} and c_{Co}^{2+} (from left to right) = 50, 100, 150 mmol·L^{-1}, respectively.

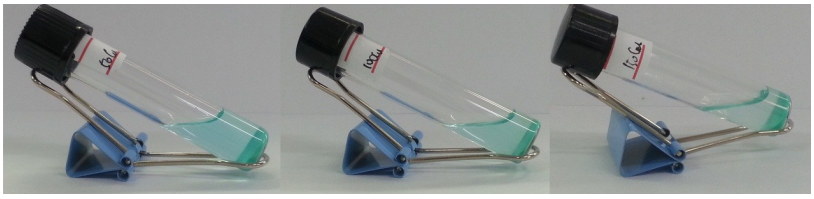

Fig. S4 Photographs of typical samples after 48 h. c_{NDC} = 100 mmol·L^{-1} and c_{Cu}^{2+} (from left to right) = 50, 100, 150 mmol·L^{-1}, respectively.

Fig. S5 Photographs of typical samples after 48 h. c_{NSA} = 100 mmol·L^{-1} and c_{Fe}^{3+} (from left to right, from top to bottom) = 50, 75, 100, 125, 150 mmol·L^{-1}, respectively.

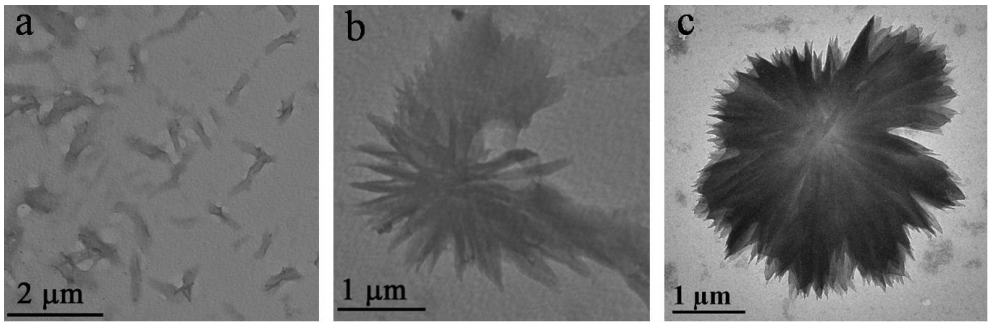

Fig. S6 TEM images of MOG formation of 100 mmol·L^{-1} NDC and 50 mmol·L^{-1} Fe^{3+} at different times: 24 h (a), 36 h (b), and 48 h (c).

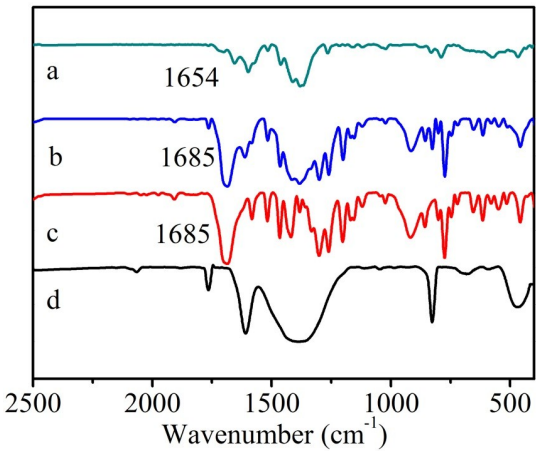

Fig. S7 FT-IR spectra of MOGs (a), mixture of $Fe(NO_3)_3$ and NDC (b), NDC (c), $Fe(NO_3)_3$ (d).

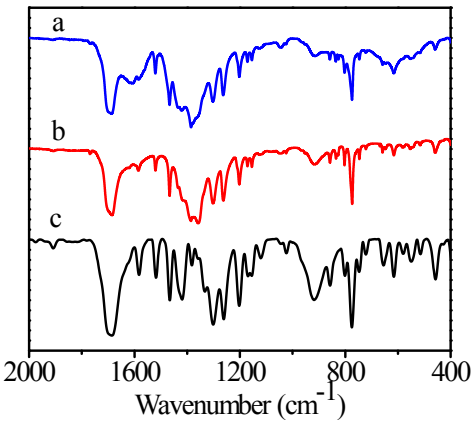

Fig. S8 FT-IR spectra of Al-NDC (a), Co-NDC (b), and NDC (c).

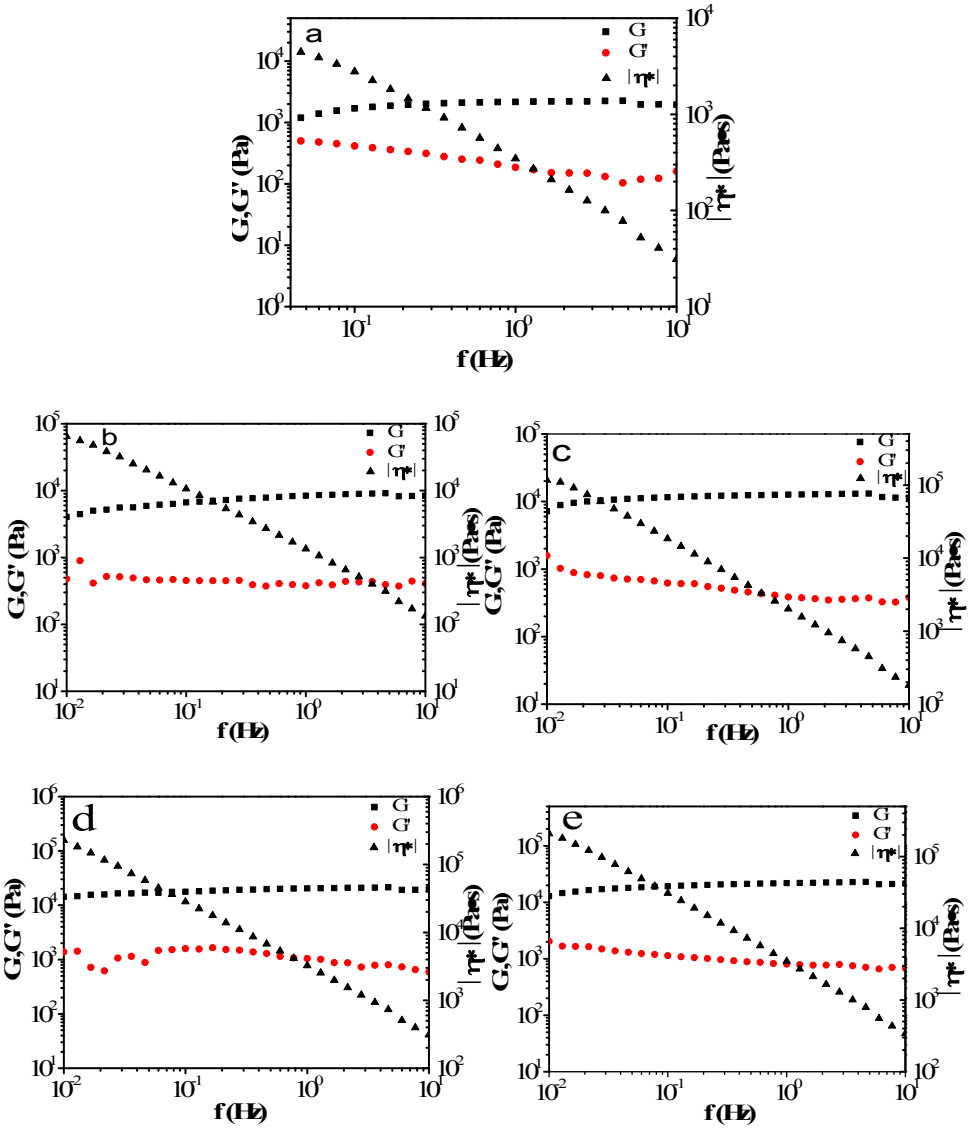

Fig. S9 Dynamically rheological results of typical samples of Fe-NDC MOGs. The c_{NDC} is 100 mmol·L^{-1} and $c_{Fe^{3+}}$: 50 (a), 75 (b), 100 (c), 125 (d), and 150 mmol·L^{-1} (e), respectively.

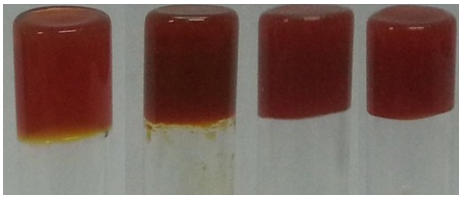

Fig. S10. Photographs of 100 mmol·L^{-1} NDC/100 mmol·L^{-1} Fe^{3+} MOGs formed in (from left to right) n-propyl alcohol, n-Butyl alcohol, EtOH/H_2O, DMF/H_2O after 24 h, respectively.

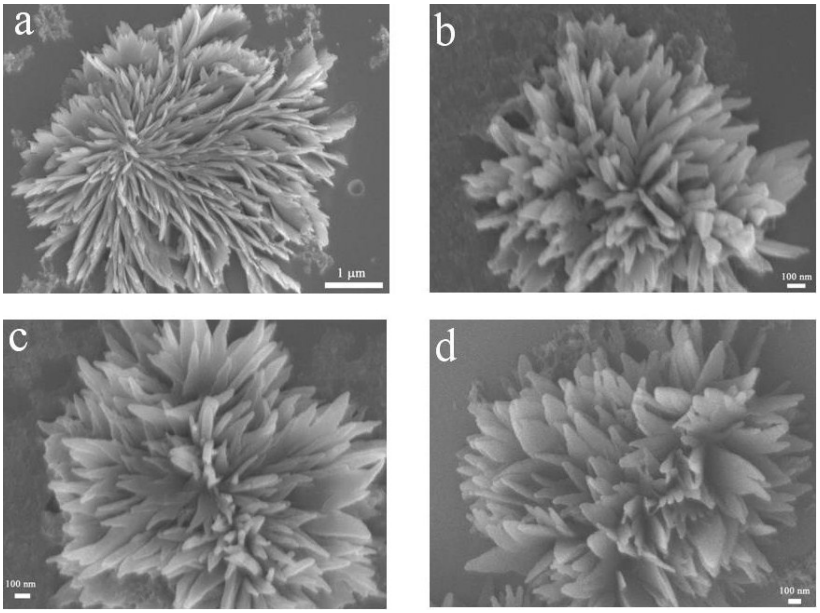

Fig. S11 SEM images of MOG formation of 100 mmol·L^{-1} NDC and 50 mmol·L^{-1} Fe^{3+} after 24 h in n-propyl alcohol (a), n-butyl alcohol (b), EtOH/H_2O (c), DMF/H_2O (d).

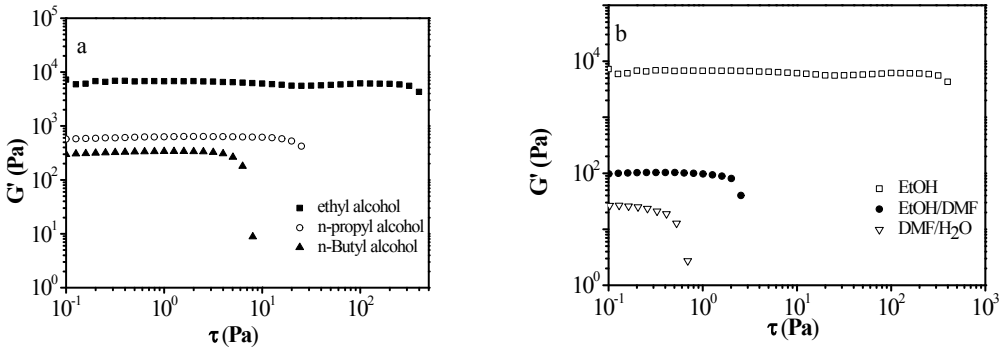

Fig. S12 Elastic modulus (G') as a function of oscillatory stress with different solvents, (a) EtOH, n-propyl alcohol, n-Butyl alcohol, (b) EtOH, EtOH/H_2O, DMF/H_2O.

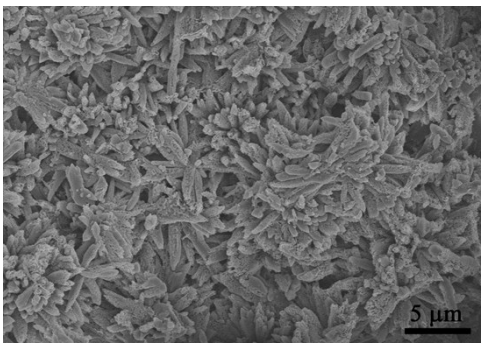

Fig. S13 SEM image of MOG after freezing drying.

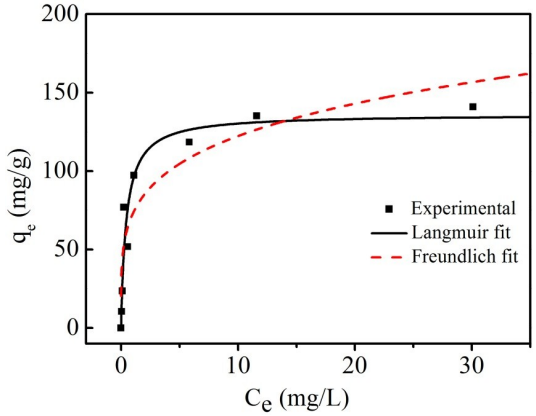

Fig. S14 Langmuir and Freundlich isotherms. pH = 7.0±0.1, $m_{xerogel}$ = 10 mg, T = 298 K.

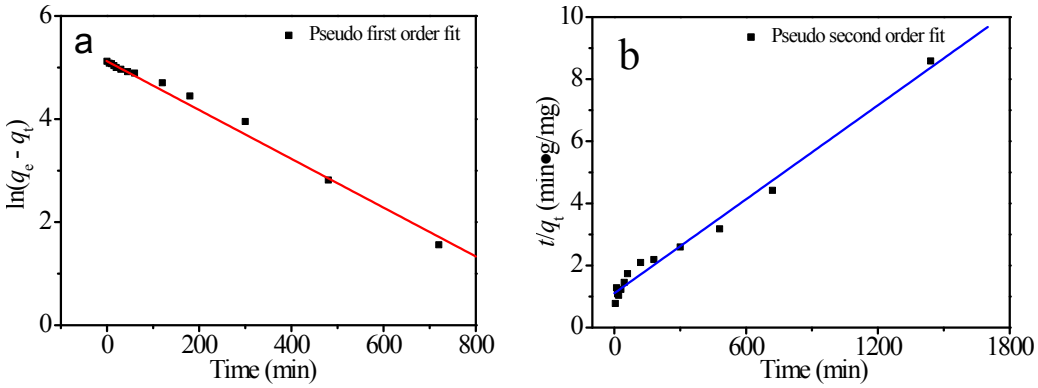

Fig. S15 (a) Pseudo-first-order and (b) pseudo-second-order plotsfor arsenic adsorption. Volume: 250 mL, initial As (V) concentration: 30 mg·L^{-1}, pH = 7.0 ±0.1, $m_{xerogel}$ = 50 mg, T = 298 K.

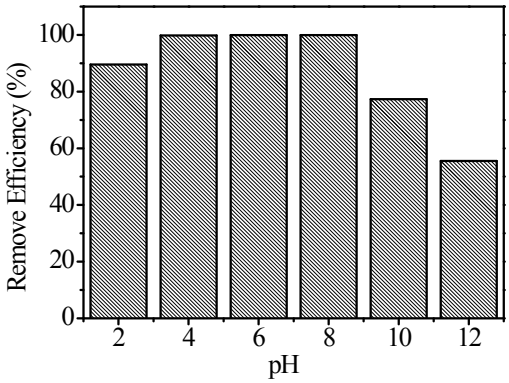

Fig. S16 Effect of pH on As (V) adsorption (volume: 50 mL, initial As concentration: 5 mg·L^{-1}, $m_{xerogel}$ = 10 mg, T = 298 K, equilibrium time = 24 h).

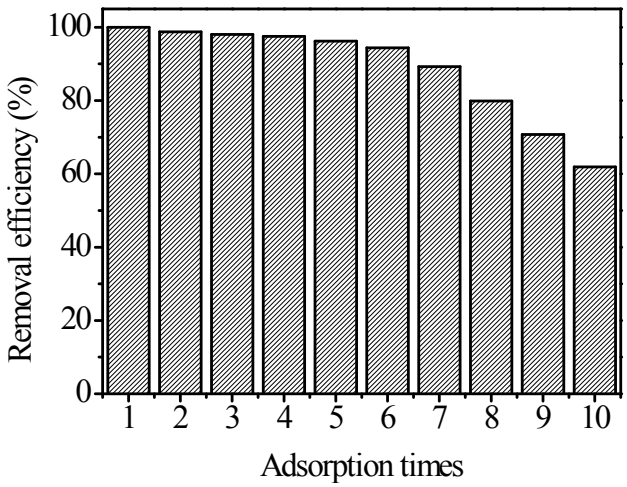

Fig. S17 Re-adsorption of arsenite by xerogel (volume: 50 mL, initial As concentration: 5 mg·L^{-1}, $m_{xerogel}$ = 10 mg, T = 298 K, equilibrium time = 24 h).

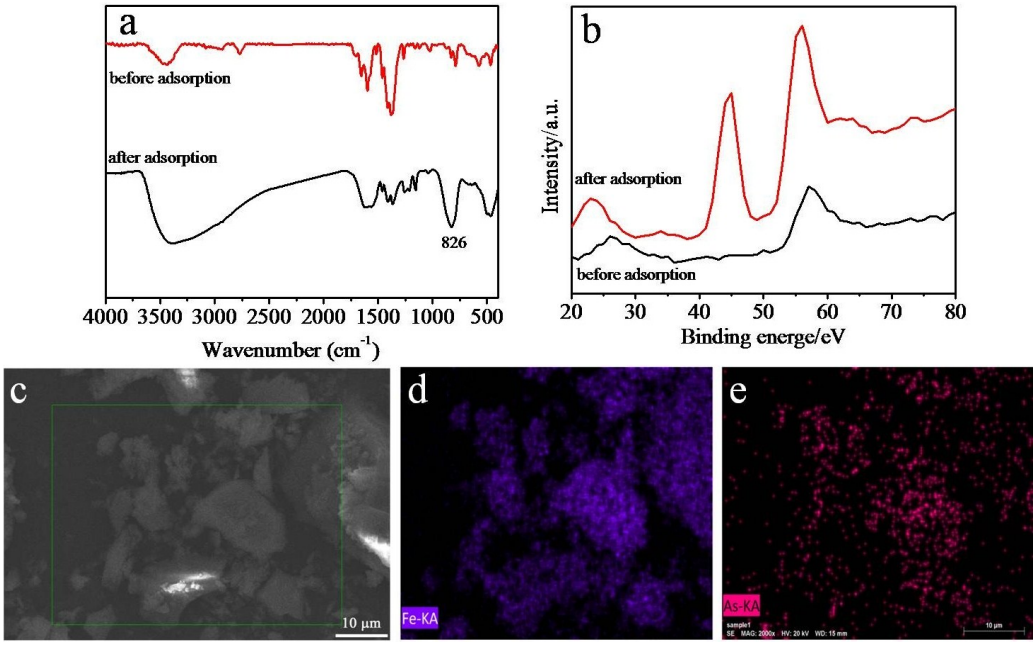

Fig. S18 (a) FT-IR spectra of xerogels before (red) and after (black) adsorption, (b) XPS spectra of xerogel before (black) and after (red) adsorption, (c) SEM image of xerogel after adsorption, (d) and (e) corresponding phase mappings of Fe Kα1 and As Kα1, respectively.

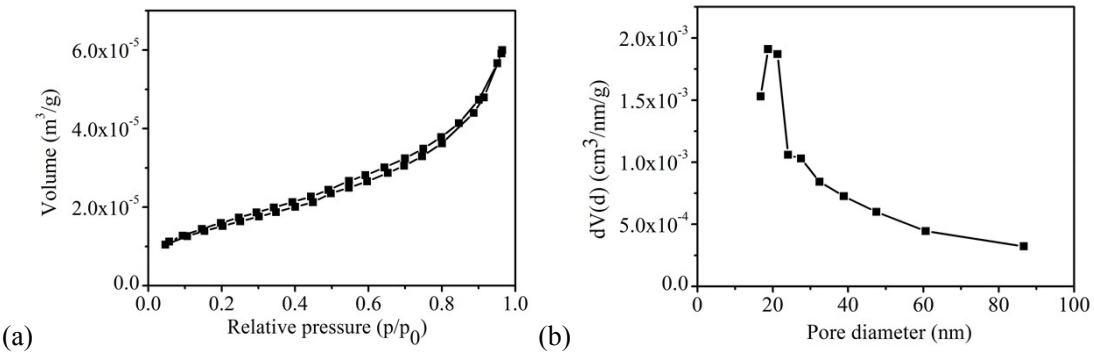

Fig. S19 The specific surface-area (a) and pore-size distribution (b) of xerogels. The isotherm is type II of five types of adsorption isotherms in the classification of Brunauer, Emertt, and Teller.[5,6] The hysteresis is of type H3, suggesting the presence of slit-type pores.

Table S1 The arsenic removal rate by MOGs and the residual concentration of arsenic.

Initial concentration ($mg \cdot L^{-1}$)	Residual concentration ($mg \cdot L^{-1}$)	Removal rate (%)
2	0.0031	99.85
5	0.0042	99.92
10	0.24	97.6
15	0.568	96.21
20	1.118	94.41
30	5.844	80.52
40	11.608	70.98
60	30.114	49.81

Table S2 Comparison of adsorption capacity of arsenic on various adsorbents.

Adsorbents	Equilibrium concentration ($mg \cdot L^{-1}$)	pH	Specific surface-area ($m^2 \cdot g^{-1}$)	Sorption capacity ($mg \cdot g^{-1}$)	Refs. in text
Fe-NDC MOGs	0.05	7	55	144	This work
Fe-Mn binary oxide	1.9	7	N/A	63.8	30
Zr-loaded resin	0.2	7	N/A	19.5	31
Nanocrystalline TiO_2	0.15	7	330	11.2	32
Fe-BTC polymer	N/A	7	N/A	12.287	33
Fe_2O_3 nanoparticles	N/A	7	N/A	6.365	33
Bulk Fe_2O_3 powders	N/A	7	N/A	1.098	33

Table S3 Parameters of pseudo-first-order and pseudo-second-order models.

pseudo-first-order			pseudo-second-order			
q_m / mg•g^{-1}	k_1 / min^{-1}	R^2	q_m / mg•g^{-1}	h / mg•min^{-1}	k_2 / mg•g•min^{-1}	R^2
167.72	0.004730	0.9994	198.0200	0.9042	2.300×10^{-5}	0.9846

Table S4 Arsenic speciation in different pH[7].

pH	< 2.3	2.3-6.9	6.9-11	> 11
Arsenic speciation	H_3AsO_4	$H_2AsO_4^-$	$HAsO_4^{2-}$	AsO_4^{3-}

Table S5. Zeta potential of MOGs at pH = 7.

c_{Fe}^{3+} (mM)	Zeta potential (mV)
50	+42.78 ±0.72
75	+49.11 ± 2.13
100	+67.10 ± 0.40
125	+70.91 ± 0.21
150	+77.28 ± 0.36

References

1 I. Langmuir, *J. Am. Chem. Soc.* 1916, **38**, 2221.

2 H. M. F. Freundlich, *J. Phys. Chem*. 1906, **57**, 385.

3 S. Lagergren, About the theory of so-called adsorption of soluble substances. **1898**.

4 Y. S. Ho and G. McKay, *Proc. Biochem.* 1999, **34**, 451.

5 M. Khalfaoui, S. Knani, M. A. Hachicha, A. B. Lamine, *J. Colloid Interface Sci.* 2003, **263**, 350.

6 C. Tien, Adsorption calculation and modeling, in: series in chemical engineering, Butterworth–Heinemann, London, 1994.

7 B. Zhu, X. Yu, Y. Jia, F. Peng, B. Sun, M. Zhang, T. Luo, J. Liu and X. Huang, *J. Phys. Chem*. *C* 2012, **116**, 8601.